

## Optical Interconnection Using Binary Phase Holograms

Myung Soo Kim

Department of Electronic Engineering  
College of Engineering, Kunsan National University  
Cheonbuk, Korea

### ABSTRACT

A block quantized binary phase hologram is introduced for optical interconnection and encoded with a simulated annealing algorithm to achieve high diffraction efficiency and suppression of unwanted spots. The block quantized binary phase holograms encoded with the algorithm are fabricated with electron beam lithography and chemical etching. The fabricated holograms showed excellent performances for optical interconnection.

### I. Introduction

Binary phase holograms (BPHs) have been successfully used for optical interconnection as well as optical pattern recognition. When BPHs are used for optical pattern recognition as a binary phase only filter<sup>(1) - (4)</sup>, they show excellent recognition performance. For optical interconnection (OI) BPHs are attractive for the ease with which they may be fabricated using standard VLSI techniques.

OIs are used to transfer data between designated points by means of optical signals<sup>(5),(6)</sup>. Fabrication technology of electronic devices has increased device densities and the speed of VLSI. As the device density increases, communication between devices and placement become difficult for two - dimensional electrical interconnection topology<sup>(7)</sup>. Pin limitations of VLSI limit communication between VLSI chips. OIs have been investigated to overcome these problems by use of three dimensional interconnection topology through optics. Also optical interconnection, using the massive parallelism that is a natural characteristics of optics, have been studied for multiprocessor system<sup>(8)</sup>.

There are several different methods for optical

interconnection using fiber optics, integrated optics, lenslet arrays, or free space interconnection. Each of them has its own advantages and disadvantages<sup>(7)</sup>. There are two methods for free space interconnection through BPHs, using Fresnel diffraction and Fraunhofer diffraction. Fresnel zone plates (FZPs) are the fundamental structure for OIs using Fresnel diffraction. But FZPs produce one to one interconnection, so one to many or global interconnection cause encoding problems for FZPs. OIs with Fraunhofer diffraction<sup>(6),(10)</sup> are good for global interconnection, but require a Fourier transform lens. Encoding of BPHs for OIs using Fraunhofer diffraction will be covered in this paper.

BPHs have good characteristics for optical interconnection, including high diffraction efficiency and ease of fabrication. However, they generate two fold rotation symmetric images, i.e., they diffract a beam into negative orders as well as positive orders. Such a property may decrease signal to noise ratio and waste optical power if one of the orders is not wanted. If the hologram for OIs is encoded with more than two phase levels, or multiphases, the unwanted orders can be eliminated,

but hologram fabrication is significantly more complicated. We introduce a relatively simple method to minimize the optical power diffracted to the unwanted orders of the BPH. This involves adding a fixed phase shift to large groups of pixels in the BPH as in Fig. 1. We call this structure a block quantized binary phase hologram (BQBPH). A simulated annealing (SA) algorithm is used to determine the block phase shift as well as the binary pixel phase pattern in the BQBPH. The encoded BQBPH will be fabricated with electron beam lithography<sup>(11)</sup> and chemical etching.

II. Encoding of BQBPH with SA algorithm

Let us represent BQBPH in Fig. 1 as follows ;

$$\begin{aligned} H(u,v) &= H_1(u,v) && \text{for upper part} \\ &= H_2(u,v) && \text{for lower part} \end{aligned} \quad (1)$$

where

$$\begin{aligned} H_1(u,v) &= [1-\exp(j\phi_1)] B_1(u,v) + \exp(j\phi_1) \\ H_2(u,v) &= \exp(j\phi_2)[1-\exp(j\phi_1)] B_2(u,v) \\ &\quad + \exp(j(\phi_2 + \phi_1)) \end{aligned} \quad (2)$$

where  $B_1(u,v)$  and  $B_2(u,v)$  are 0 or 1. So, for the upper part of the BQBPH,

$$\begin{aligned} H_1(u,v) &= 1 && \text{for } B_1(u,v) = 1 \\ &= \exp(j\phi_1) && \text{for } B_1(u,v) = 0 \end{aligned}$$

and for the lower part,

$$\begin{aligned} H_2(u,v) &= \exp(j\phi_2) && \text{for } B_2(u,v) = 1 \\ &= \exp(j(\phi_2 + \phi_1)) && \text{for } B_2(u,v) = 0 \end{aligned}$$

The phase of pixels in the lower part of BQBPH is uniformly shifted by  $\phi_2$ . When  $H_1(u,v)$  consists of  $K_1 \times L$  square pixel,  $H_2(u,v)$  consists of  $K_2 \times L$  square pixels and  $H(u,v)$  is replicated in the  $(u,v)$  domain, Fourier series coefficients  $h_{mn}$  of the replicated BQBPH are amplitudes in the frequency domain. Thus,  $|h_{mn}|^2$  represents intensities of spots at the back plane of Fourier transform lens when the BQBPH is at the front focal plane of the lens.

The SA algorithm<sup>(13)</sup> is an iterative algorithm to find a global minimum energy of a system through perturbing system variables and decreasing a temperature parameter. In BQBPH encoding  $B_1$ ,  $B_2$ ,  $\phi_1$ , and  $\phi_2$  are defined to be the system variables. The system energy function is formulated to give a global minimum energy when the intensities in the spot array are equal, the diffraction efficiency is high, and the intensities of unwanted spots are suppressed. Thus, the energy function  $E$  that we used is

$$\begin{aligned} E &= \sum \sum D_{mn} (1/MN - |h_{mn}|^2)^2 + A(P_{max} - P_{min})^2 \\ &\quad + \sum \sum S_{mn} |h_{mn}|^2 \end{aligned}$$

where  $MN$  is total number of desired spots,  $D_{mn}$  is a weight factor for equal intensity and high diffraction efficiency,  $P_{max}$  is the highest intensity among the desired spots,  $P_{min}$  is the lowest intensity among the desired spots,  $A$  is a weight factor to minimize intensity difference between the desired spots and  $S_{mn}$  is a weight factor to suppress the intensities of the unwanted spots. The rate of temperature decrease used is

$$T = (D_T)^r T_{initial} \text{ and } D_T = (T_{final} / T_{initial})^{1/q}$$

where  $r$  is iteration index,  $q$  is the total number of the iteration and  $D_T > 0.9$ . An iteration is considered to be one updating of all pixels.

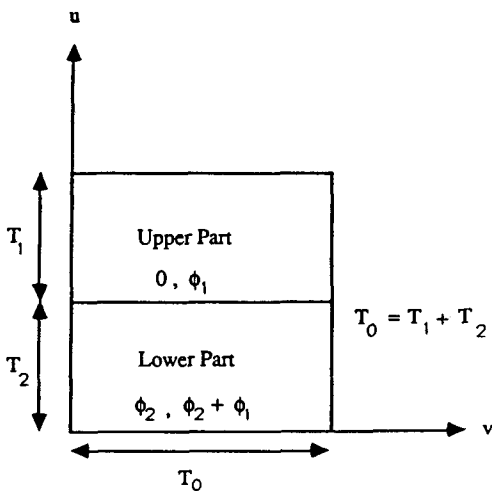


Fig. 1 Block quantized binary phase hologram

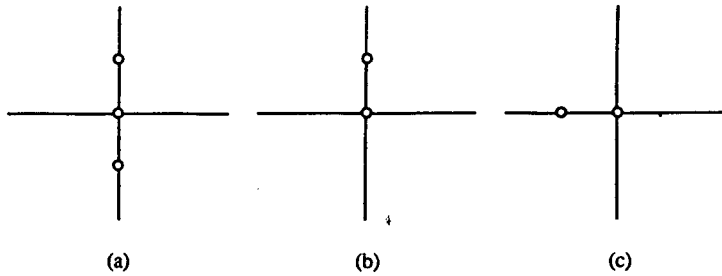


Fig. 2. Spot arrays of group 1. Circles represent locations of the spots. The center spot is (0,0) order, the upper spot is (0,1) order, the left spot is (-1,0) order and so on.

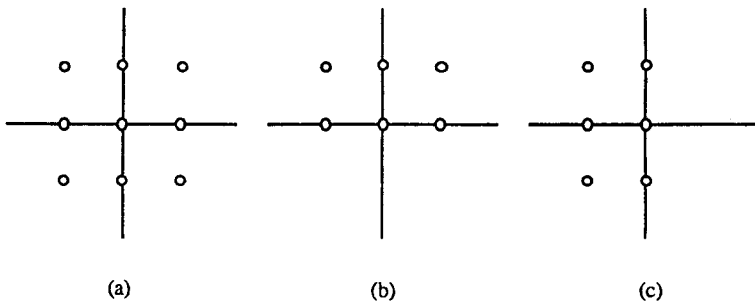


Fig. 3. Spot array of group 2. The upper left circle represents (-1,1) order, the upper right represents (1,1) order, the center represents (0,0) order, and so on.

### III. Computer simulation

The upper half block of the BQBPH in Fig. 1 consists of  $23 \times 45$  pixels while the lower half consists of  $22 \times 45$  pixels. Two groups of spot arrays in the computer simulation are considered as shown in Figs. 2 to 4. Each group includes a two fold rotation symmetric array as well as asymmetric arrays. For each array, two phases  $\phi_1$  and  $\phi_2$  that give not only high diffraction efficiency and uniform intensities of the desired spots in the array but also suppression of the unwanted spots are obtained using the SA algorithm. The phases,  $\phi_1$  and  $\phi_2$ , total diffraction efficiency (TDE) of a spot array, average diffraction efficiency (DE),

intensity nonuniformity (INU), and suppression ratio are summarized in Table I. INU, introduced as a measure of nonuniformity of the intensities of the wanted spots is defined as

$$INU = (P_{\max} - P_{\min}) / P_{\text{ave}} \times 100 (\%)$$

where  $P_{\text{ave}}$  is the average intensity. The suppression ratio, introduced as a measure of how much the intensities of the unwanted spots are suppressed with regard to the wanted spots, is defined as  $SR = P_{\text{ave}} / P_{\text{sumax}}$  where  $P_{\text{sumax}}$  is the highest intensity among the unwanted spots. Computation time for each array was around 200 minutes on Celerity.

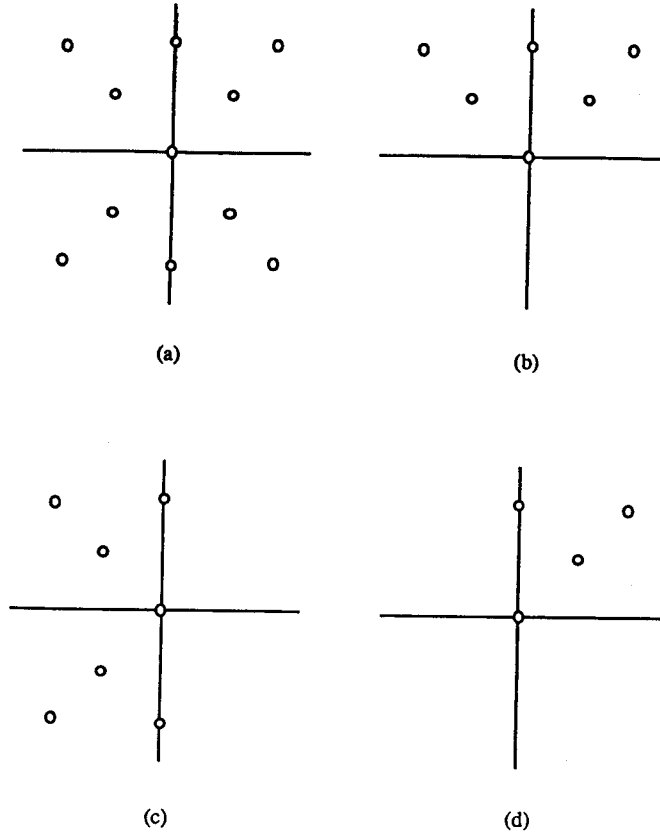


Fig. 4. Spot array of group 3. The upper right circle is (-2,2) order, the upper right is (2,2) order, the lower right is (2,-2), the center is (0,0) and so on.

#### IV. Fabrication of BQBPH

Three BQBPHs for the spot arrays in Fig. 4 (b) to (d) were fabricated using an e - beam lithography system made by Cambridge Instruments. The e - beam masks we used are low expansion glass with a 1000 angstrom layer of chrome on one surface. Each BQBPH is replicated 10 x 10 times. The size of the pixel in the BQBPH is 20 x 20 microns so that total size of each BQBPH is 9 x 9 mm. Quartz plates are used for the actual surface relief BQBPHs. They are cleaned according to the procedures for silicon wafers. Photoresist is then spun on them. The plate and the e - beam mask are aligned with a mask aligner and exposed with UV light.

There are several etching techniques, but we used chemical etching which is the easiest one among them. The etching depth  $L$  of BPOF is calculated as follows :

$$L = \lambda \phi / 2\pi(n - 1)$$

where  $\lambda$  is the wavelength of a laser,  $n$  is the refractive index of the quartz plate, and  $\phi$  is the binary phase. For He - Ne laser,  $\lambda = 6328$  angstrom and  $n \approx 1.465$ , and  $\phi$  is the phase as in Table I.

#### V. Optical experiments and their results

The optical system used for the OI with fabricated BPOFs is shown in Fig. 5. BQBPH is at the front focal plane of Fourier lens. A TV camera at

Table I. Results of computer simulation for various spot arrays.

SRs of the symmetric arrays are marked with \* .

spot arrays	phases (radians)		TDE (%)	DE (%)	INU (%)	SR
	$\phi_1$	$\phi_2$				
Fig. 2 a	0.28	4.35	88.1	29.4	3.2	*
Fig. 2 b	1.03	1.72	75.2	37.6	0.3	17.2
Fig. 2 c	4.93	5.32	56.0	28.0	7.5	3.9
Fig. 3 a	4.26	4.30	75.6	8.4	7.9	*
Fig. 3 b	2.38	4.31	63.0	10.5	5.7	111.7
Fig. 3 c	4.26	4.55	52.8	8.8	1.9	1.7
Fig. 4 a	2.92	0	75.2	6.84	4.4	*
Fig. 4 b	2.69	1.06	41.1	6.85	7.3	3.6
Fig. 4 c	3.46	0.90	44.7	6.39	4.7	2.4
Fig. 4 d	2.54	1.12	40.4	10.1	3.0	5.0

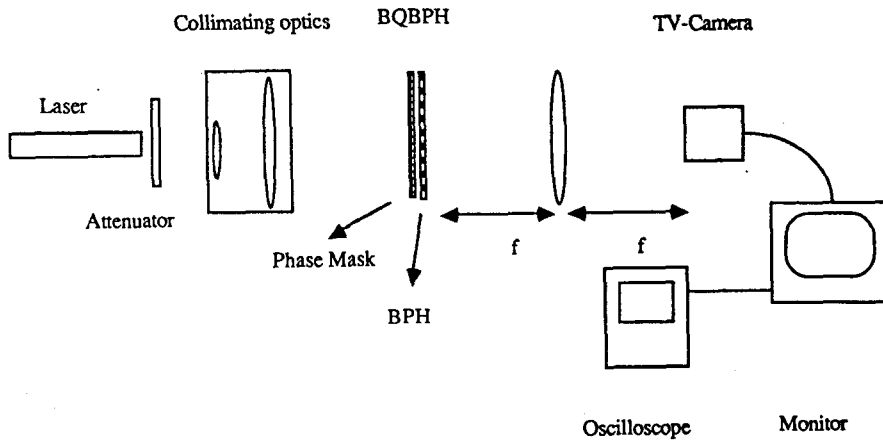


Fig. 5 Optical system for experiment

the back focal plane of the lens is connected to a TV monitor to observe the intensities of the spots. The video signal from the TV monitor is sent to an oscilloscope to measure quantitatively the outputs. The TV camera, TV monitor, and oscilloscope system respond nonlinearly to high intensities and easily saturated. This is corrected for the high intensities. The numerical values of the intensities in each spot array taken from the oscilloscope trace are summarized in Fig. 6.

VI. Conclusion

A conventional binary phase hologram generates negative orders as well as positive orders. If one of the orders is not wanted for optical interconnection, it wastes optical power and increases noise. BQBPH which is relatively easy to fabricate is introduced to overcome these problems. BQBPHs are encoded with a simulated annealing algorithm and the encoded BQBPHs are fabricated using electron beam lithography and chemical etching. The fabricated BQBPHs showed excellent performance for optical interconnection.

References

1. J. L. Horner and J. R. Leger, Appl. Opt., vol. 24, pp. 609-611, 1985
2. D. Psaltis, E. G. Peak, and S. S. Venkatesh, Opt. Eng., vol. 23, pp. 698-704, 1984
3. D. M. Cottrell, R. A. Lilly, J. A. Davis, and T. Day, Appl. Opt., vol. 26, pp. 3755-3761, 1987
4. M. W. Farn and J. W. Goodman, Appl. Opt., vol. 27, pp. 4431-4437, 1988
5. J. W. Goodman, F. I. Leonberg, S. Y. Kung, and R. A. Athale, Proc. SPIE, vol. 72, pp. 479-481, 1989
6. M. R. Feldman and C. C. Guest, Opt. Lett., vol. 14, pp. 479-481, 1989
7. D. G. Feitelson, Optical Computing, The MIT press, 1988
8. B. K. Jenkins, P. Chavel, R. Forchheimer, A. A. Sawchuck, and T. C. Strand, Appl. Opt., vol. 23, pp. 3465-3474, 1984
9. M. R. Feldman and C. C. Guest, Opt. Eng., vol. 28, pp. 915-921, 1989
10. H. Damman and E. Klotz, Opt. Act., vol. 24, pp. 505-515, 1977
11. S. M. Arnold, Opt. Eng., vol. 24, pp. 803-807, 1985
12. J. A. Davis, G. W. Bach, D. M. Cottrell, and R. A. Lilly, Appl. Opt., vol. 27, pp. 2949-2953, 1988
13. S. Kirkpatrick, C. D. Gelatt, J. A. Davis, and T. Day, Science 220, pp 671-679, 1983

53 * 71 * 78	29 * 42 * 13	* * 37 * 31
* 93 * 100 *	* 29 * 10 *	* * * 55 *
* * 78 * *	* * 100 * *	* * 100 * *
* 16 * 18 *	* 23 * 13 *	* 9 * * *
10 * 19 * 14	23 * 31 * 10	9 * 9 * *
(a)	(b)	(c)

Fig. 6 Numerical data of the optical experiments from the oscilloscope traces for the spot arrays in Fig. 4 (b) to (d). \* is the location of the spot which is not considered in the energy function during annealing process.